STUDYING ZINC OXIDE/COPPER OXIDE/CADMIUM SELENIDE NANOSTRUCTURES FOR LIGHT EMITTING DIODES

ESTUDIO DE NANOESTRUCTURAS DE ÓXIDO DE ZINC/ÓXIDO DE COBRE/SELENIURO DE CADMIO PARA DIODOS EMISORES DE LUZ

Zehraa N. Abdul-Ameer

University of Baghdad, College of science, Nanotechnology, Remote Sensing and GIS, Iraq.

(Recibido: jun./2024. Aceptado: oct./2024)

Abstract

The synthesis of zinc oxide, copper oxide, and cadmium selenide as a heterostructure was conducted using a simple co-precipitation method. Structural, optical, and electrical properties were investigated. XRD patterns show hexagonal form for ZnO, cubic for CuO, and wurtzite for CdSe, with an average particle size of 18.5, 22.3, and 38.2 nm for ZnO, CuO, and CdSe, respectively. SEM images show ZnO crystals with a nanorod shape and CuO and CdSe nanoparticles with nano-branch agglomerations in all directions. Optical properties exhibit a redshift in absorbance (460 nm) with photoluminescence peaks at 500 nm for the heterostructure and a broadened band gap (2.5 eV). In light, the heterostructure shows increased light absorption, leading to enhanced electron-hole production and an exponential increase in forward current. These results enhance the success of fabrication of high-amplification light-emitting diodes.

Keywords: zinc oxide, copper oxide, cadmium selenide, nanostructures, light-emitting diode.

zehraa.najim@sc.uobaghdad.edu.iq doi: https://doi.org/10.15446/mo.n70.114898

Resumen

Se sintetizó óxido de zinc, óxido de cobre y seleniuro de cadmio como heteroestructura utilizando el método de co-precipitación simple. Se investigaron las propiedades estructurales, ópticas y eléctricas. Los patrones de DRX muestran una forma hexagonal para el ZnO, cúbica para el CuO y de wurtzita para el CdSe, con un tamaño de partícula promedio de 18.5, 22.3 y 38.2 nm para ZnO, CuO y CdSe, respectivamente. Las imágenes de SEM muestran cristales de ZnO en forma de nanovarilla y nanopartículas de CuO y CdSe con nano-ramas aglomeradas en todas las direcciones. Las propiedades ópticas exhiben un desplazamiento al rojo en la absorbancia (460 nm) con picos de fotoluminiscencia a 500 nm para la heteroestructura y una brecha de banda ampliada (2.5 eV). Bajo la luz, la heteroestructura muestra una mayor absorción, lo que conduce a un aumento en la producción de pares electrón-hueco y a un incremento exponencial de la corriente de avance.

Palabras clave: óxido de zinc, óxido de cobre, seleniuro de cadmio, nanoestructuras, diodo emisor de luz.

Introduction

Nanoparticle structures are new materials with superior structural, optical, and electrical properties. These properties make them suitable for various applications such as optoelectronics, photodetectors, and light-emitting diodes [1].

Zinc oxide nanoparticles are interesting semiconductors with a band gap of 2.9-3 eV that have unique properties which make them distinct for gas sensors [2], UV-blue light emitters, and transistors [3]. ZnO has structural and optical properties with high transparency, making it suitable for various applications [4]. Copper oxide (p-type) is a cheap semiconductor with a narrow band gap (1.2 eV) in bulk, monoclinic structure, and simple preparation methods [5]. CuO possesses unique electrical and optical properties for a wide range of applications, such as

supercapacitors, near-infrared filters, sensors, and semiconductors [6].

Cadmium selenide is an interesting semiconductor with notable physical, structural, optical, and electrical properties. Its unique structure with three types of crystalline forms—wurtzite, hexagonal, and cubic [7]—makes it versatile. Researchers have explored the preparation of cadmium selenide using various methods: solvothermal [8], thermal evaporation [9], and microwave-assisted methods [10], yielding promising results that make it suitable for optoelectronic applications.

This research aims to prepare Zinc Oxide/Copper Oxide/Cadmium selenide nano heterostucture using the co-precipitation method and study structural, optical, and electrical properties to explore its effectiveness for optoelectronic devices, especially light-emitting diodes.

Experimental part

(0.1 M) Hexamethylenetetramine (HMT) and equal molar ratios of zinc nitrate ($Zn(NO_3)_2{\cdot}6H_2O$) solutions were prepared in a reaction vessel. At that time, the precursor solution (zinc nitrate) was kept at 50 °C for a few hours, then heated at 600 °C for 3 hours [11].

(5 mM) Copper nitrate Tri hydrate ($(CuNO_3)_2{\cdot}3H_2O$) as precursor was dissolved in 100 ml of double deionized water with continuous stirring. 1 mM Hexamethylenetetramine (HMT) was added, followed by the addition of 10 % sodium hydroxide (NaOH) to prepare the final solution. The aqueous solution was held in an oven at 90 °C for 2 hours; a brown powder of copper oxide was obtained and heated at 450 °C for 3 hours [12].

Cadmium chloride and sodium selenide were dissolved in deionized water in equal ratios with continuous stirring for 30 minutes. 20 % of ethylene glycol (reagent volume ratio) was added. The prepared solution was held in the microwave for 45 minutes, then the mixture was filtered, cleaned, and dried at 50 °C for an hour [13]. The

prepared triple structure was formed by depositing an aqueous solution of each layer using the spin coating method, then dried and annealed in a tube furnace at 600 °C for an hour.

Results and Discussion

Laser Thickness Method

The interferometer method was used to measure the thickness of ZnO, CuO, and CdSe layers respectively by light beam reflection. A He-Ne laser source of 632.8 nm was used to calculate the thickness of each layer, as shown in Equation 1 [13].

$$d = \frac{\Delta x}{x} \cdot \frac{\lambda}{2} \tag{1}$$

Where x (fringe width), Δx (distance between two fringes). The thickness was found to be approximately 100 nm for each constituent layer. X-ray patterns were investigated using a diffractometer with Cu Kα radiation ($\lambda = 1.54056\,\text{Å}$). Scherrer's equation 2 [14] was used to determine particle size:

$$D = 0.9\frac{\lambda}{\beta \cos\theta} \tag{2}$$

Where β: full width at half maximum; θ: Bragg's angle. The average microstrain of the nanostructure, which represents the lattice disarrangement, can be estimated using equation 3[15]

$$\epsilon = \frac{\beta \cos\theta}{4} \tag{3}$$

Dislocation density is defined as the number of dislocations in a crystalline material per unit area, as shown in equation 4 [16]

$$\delta = \frac{1}{D^2} \tag{4}$$

The XRD structure parameters for each constituent structure are shown in Table 1.

Parameter	ZnO	CuO	CdSe
(hkl)	(100),(002),(102) (110),(103),(200)	(110),(002),(111), (020),(202),(220), (113)	(100),(002),(101), (110),(112),(103), (112),(203)
β (rad)	0.05	0.03	0.036
D (nm)	18.5	22.33	38.2
ε ($*10^{-3}$ lines^{-2} m^{-4})	683	565	881
δ (1/nm^2)	2.9	2	6.18

TABLE 1. *XRD parameters*

Figure 1 shows characteristic peaks for zinc oxide located at $2\theta = 31.1°$, $32.9°$, $43.4°$, $52.81°$, $60.1°$, and $66.8°$, corresponding to (100), (002), (101), (102), (110), (103), (200) with hexagonal crystal structure matching JCPDS 36-1451.

CuO patterns are at $2\theta = 18°$, $24.9°$, $33.4°$, $35.3°$, $39.1°$, $42.7°$, $49.8°$, $56.3°$, $63.1°$, $66.8°$, and $74.3°$ (cubic crystal structure), corresponding to (020), (021), (110), (002), (111), (042), (130), (131), (151), (113), (200), (152), and (202), confirmed by JCPDS 0080-1916.

Characteristic peaks for CdSe are at $2\theta = 23.45°$, $25.56°$, $27.23°$, $41.21°$, $45.7°$, $49.6°$, and $63.8°$ corresponding to (100), (002), (101), (110), (112), (103), and (203) planes, respectively. These peaks match the hexagonal (wurtzite) crystal structure as in JCPDS 00-008-0459.

SEM images were analyzed using the XL30 scanning electron microscope to study nanoparticle shapes and sizes. ZnO images show tiny nanorod-shaped crystals ($\sim$15 nm). These nanorods align vertically on the surface of the substrate. Meanwhile, CuO images show nano-branches with agglomerations of particles in all directions ($\sim$23 nm). CdSe forms large clusters with irregular distributions of granules and agglomerations in non-symmetrical directions, with a particle size of 33 nm, as shown in Figure 2.

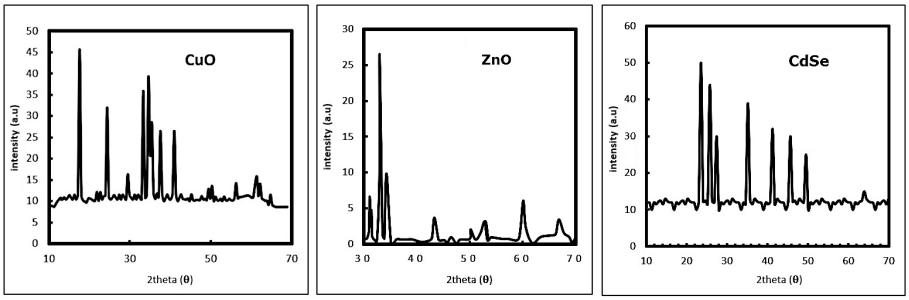

FIGURE 1. *XDR patterns*

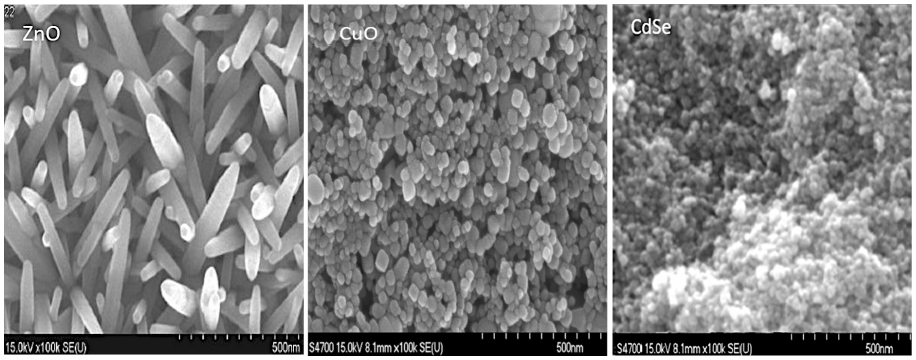

FIGURE 2. *SEM images of nanoparticles*

The UV-visible spectrum was measured using the Shimadzu instrument. Optical properties were investigated from UV-spectroscopy in the wavelength range of 200-1200 nm at room temperature. Figure 3[16] shows a plot of $(\alpha h\nu)^2$ versus $h\nu$ to calculate the energy gap. The optical band gap can be determined using the Tauc equation:

$$(\alpha h\nu) = A(h\nu - E_g)^{1/2} \tag{5}$$

A: is constant, α: absorption coefficient, h Planck's constant, ν: frequency of radiation in Hz. The energy gap is plotted in Figure 3 and was found to be approximately 3.4 eV for ZnO, 2.85 eV for CuO, and 1.9 eV for CdSe.

The tri-layer structure exhibits an energy gap of 2.5 eV. As observed, the energy gap increases as particle size decreases due

to the higher energy required to transfer electrons from the valence band to the conduction band. It is known that the energy gap is inversely related to particle size, affecting the surface area ratio. This ratio varies with particle shape, size, and the number of atoms on the surface, leading to cohesive energy [17]. Figure 3 also shows that the prepared structure (tri-layer) has a thickness of about 100 nm with a broadened band gap, which indicates the presence of photon absorption by the nanostructure.

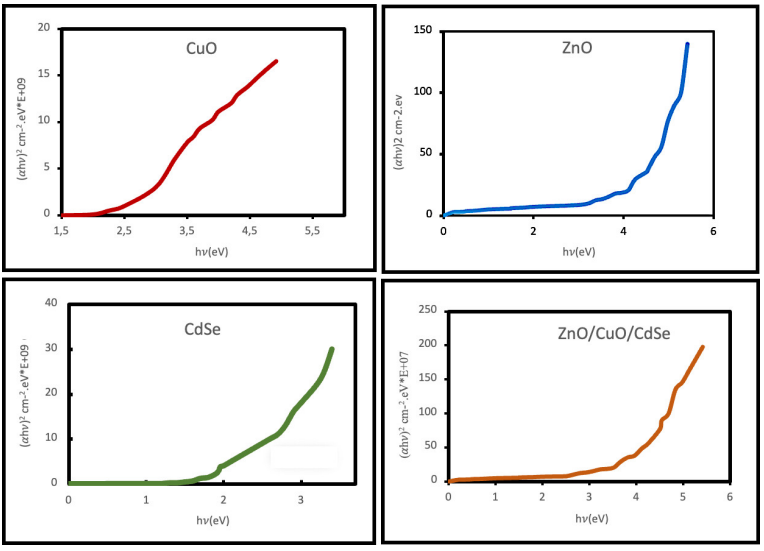

FIGURE 3. *Optical energy gap*

Figure 4 shows the absorption spectra of samples at room temperature. The wavelength was measured in the range of 200-1200 nm. For ZnO, absorption peaks are recorded at 370 nm, which is blue-shifted compared to bulk ZnO due to quantum confinement [18]. Meanwhile, CuO nanoparticles show an absorption peak at 430 nm. These results agree with previous findings that record peaks ranging between 400-600 nm [19]. CdSe shows an absorption peak at 420 nm.

The absorption edge near the absorption region indicates a direct allowed transition of CdSe nanoparticles. The absorption edge is blue-shifted compared to bulk CdSe, which was 712 nm [20]. The prepared triple structure has an absorption peak at 460 nm,

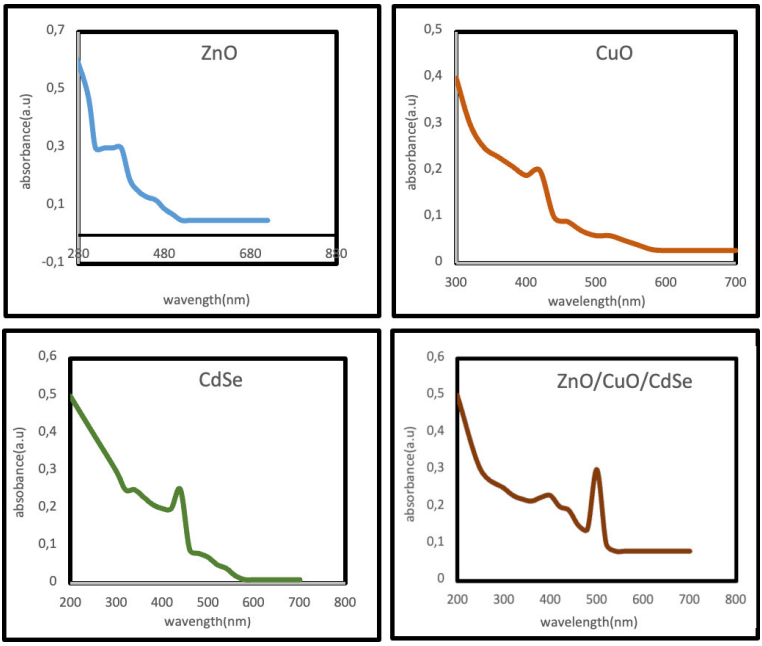

FIGURE 4. *Absorbance spectrum of samples*

suggesting its suitability for use as an LED.

Photoluminescence is an important characterization method for studying optical properties. ZnO emission spectra were studied with an excitation energy of 320 nm, and the emission peak is at 520 nm [21]. Photoluminescence bands are reported for copper oxide nanoparticles, ranging from the UV to IR region at 400 nm. Photoluminescence of CdSe shows a prominent peak, which confirms a blue shift compared to bulk, attributed to the quantum size effect [22]. Photoluminescence emission spectra for CdSe were observed at 540 nm, with a peak shifted toward green with a narrow profile, attributed to cadmium vacancies as a donor and interstitial selenium acting as an acceptor [23]. The heterostructure recorded a photoluminescence peak at 500 nm, as shown in Figure 5. The peak is located in the blue-green region. The strong PL peak indicates high crystallinity of the heterostructure. The photoluminescence results of the prepared heterostructure support the potential for utilizing this nanostructure as a light-emitting diode.

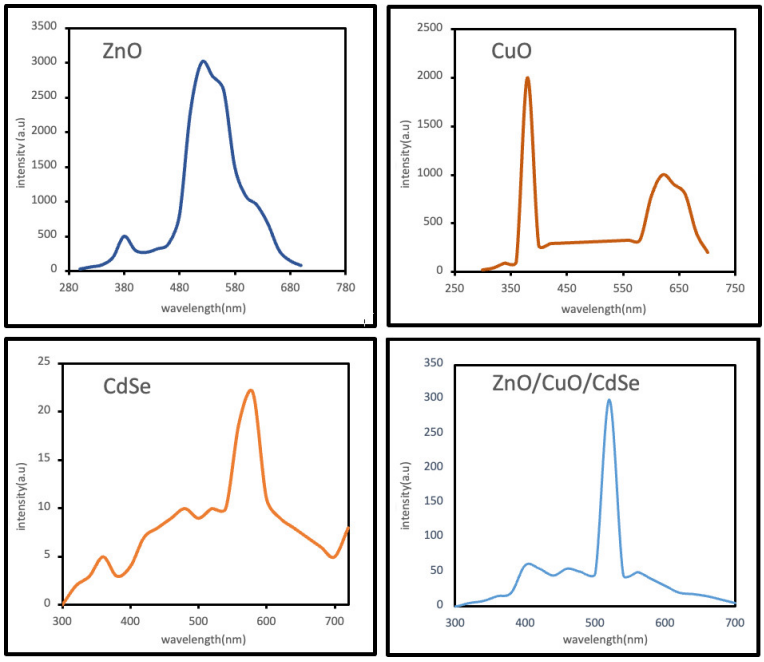

FIGURE 5. *Photoluminescence spectra*

The electronic materials play an important role in new technologies. Electrical conductivity and I-V characteristics represent an important indication for effectiveness of light-emitting diode of heterostructure, as shown in Figure 6.

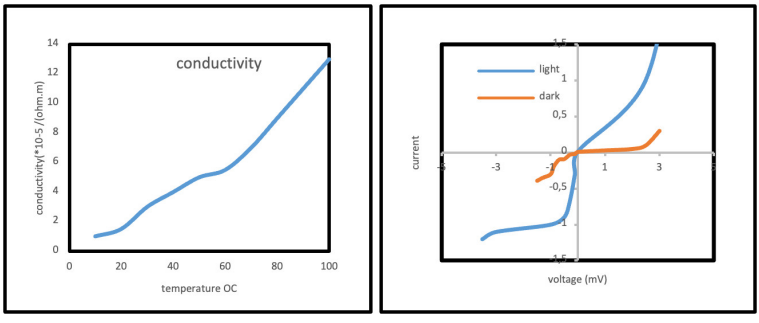

FIGURE 6. *Conductivity b- I-V characteristic*

Figure 6 illustrates the conductivity of the triple structure, which can be determined using equation 6,[24] as shown in Table 2:

$$\sigma = \frac{L}{RA} \tag{6}$$

R is the film resistance, A is the cross-sectional area, and L is the distance between electrodes. The Hall effect can be calculated using equation 7,[24] as shown in Table 2:

$$R_H = \frac{1}{Ne} \tag{7}$$

Where N is the carrier concentration (cm^3) (from I-V curve), and e is the electron charge. I-V measurements are performed under dark and light conditions at forward and reverse biases for the prepared heterostructure.

Figure 6b: At forward bias, the I-V curve starts from zero and then increases gradually. When the barrier internal voltage exceeds a certain threshold, there is an increase in forward current with nonlinear behavior. The existence of a difference between the dark and light conditions is observed as an increase in current under illumination. These results agree with CdSe behavior [24].

Parameter	**ZnO**	**CuO**	**CdSe**
Carrier concentration (cm^{-3})	(n-type) N_D=10^{17}	(p-type) $N_A = 10^{16}$	(n-type) $N_D = 2.6 \times 10^{15}$
Hall effect (cm^3/C)	-62.5	625	-240.38
Mobility (cm^2/v·sec)	12.8×10^{-2}	21.78×10^{-6}	30.2×10^{-2}
σ $(\Omega.cm)^{-1}$	6.25×10^{-3}	3.75×10^{-7}	5.25×10^{-3}

TABLE 2. *Nanostructure electrical parameters*

The sensitivity is the ability to absorb photons and generate electron-hole pairs (excitons) when the sample is exposed to light. In the dark, when voltage is applied to the heterostructure, an electric current is recorded. In the light, the absorption of light leads to an increase in electron-hole production, which increases current exponentially in forward bias, as shown in Figure 7. These results indicate the success of the fabrication of a high-amplification light-emitting diode [25].

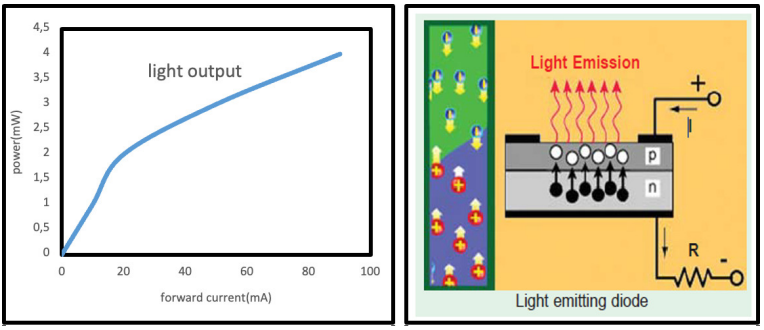

FIGURE 7. *Power light output*

Conclusion

A simple co-precipitation method was used to synthesize a triple-layer heterostructure of zinc oxide, copper oxide, and cadmium selenide. XRD patterns show hexagonal form for ZnO, cubic for CuO, and wurtzite for CdSe, with average particle sizes of 18.5 nm, 22.3 nm, and 38.2 nm for ZnO, CuO, and CdSe, respectively. SEM images show crystals of nanorod shape for ZnO and nano-branches with agglomeration of particles in all directions for CuO and CdSe nanoparticles. Optical properties show a red shift in absorbance (460 nm) with strong photoluminescence peaks (500 nm) of the heterostructure and a broadened band gap (2.5 eV). In light, the heterostructure shows the absorption of light, which leads to an increase in electron-hole production and an exponential increase in current at forward bias. Optical, structural, and electrical results of the heterostructure enhance the success of the fabrication of high-amplification light-emitting diodes.

References

[1] Y. Zhu and X. Wu, Prog. Mater. Sci. **131**, 101019 (2023).

[2] C. Pushpalatha, J. Suresh, and et al., Front Bioeng Biotechnol. **19**, 917990 (2022).

[3] Z. Abdul-Ameer, Iraqi J. Sci. **65**, 2460 (2024).

[4] A. Katiyar, N. Kumar, and et al., Mater. Today - Proc. **46**, 2374 (2021).

[5] M. Grigore, E. Biscu, and et al., Pharmaceuticals **9**, 75 (2016).
[6] M. Sahooli, S. Sabbaghi, and R. Saboori, Materials Letters **81**, 169 (2012).
[7] P. Sanjay, K. Deepa, and et al., IOP Conf. Ser.: Mater. Sci. Eng. **360**, 012010 (2018).
[8] S. Sagadevan and C. Arunseshan, Appl. Nanosci. **4**, 179 (2014).
[9] G. Ramalingam, N. Melikechi, and et al., J. Cryst. Growth **311**, 3138 (2009).
[10] M. Ali, W. Syed, and et al., Appl. Surf. Sci. **284**, 482 (2013).
[11] L. Roza, K. Fairuzy, and et al., J. Mater. Sci.: Mater. Electron. **26**, 7955 (2015).
[12] Z. Abdul-Ameer, Momento **68**, 27 (2024).
[13] Z. Abdul-Ameer, J. Opt. **53**, 5065 (2024).
[14] Z. Abdul-Ameer, Momento **67**, 67 (2023).
[15] D. Nath, F. Singh, and R. Das, Mater. Chem. Phys. **239**, 122021 (2020).
[16] J. Al Abbas, L. Al Taan, and M. Uonis, Chalcogenide Lett. **20**, 883 (2023).
[17] M. Singh, M. Goyal, and K. Devlal, J. Taibah Univ. Sci. **12**, 470 (2018).
[18] D. Singh, D. Pandey, and et al., Pramana - J. Phys. **78**, 759 (2012).
[19] A. Kudhur, A. Salim, and et al., J. Opt. **53**, 1936 (2024).
[20] A. Layashchova, A. Dmytruk, and et al., Nanoscale Res. Lett. **9**, 88 (2014).
[21] R. Zhang, P.-G. Yin, and et al., Solid State Sci. **11**, 865 (2009).
[22] S.-S. Chang, H.-J. Lee, and H. J. Park, Ceramics International **31**, 411 (2005).
[23] J. Yu and R. Chen, InfoMat. **2**, 905 (2020).
[24] K. K. Pathak, M. A. Pateria, and et al., Materials Science-Poland **37**, 33 (2019).
[25] P. Bai, A. Hu, and et al., The Journal of Physical Chemistry Letters **13**, 9051 (2022).